Progress In Electromagnetics Research C, Vol. 59, 135–141, 2015

Compact Microstrip Magnetic Yagi Antenna and Array with Vertical Polarization Based on Substrate Integrated Waveguide

Zhao Zhang*, Xiangyu Cao, Jun Gao, Sijia Li, and Xiao Liu

Abstract—A compact magnetic Yagi antenna and a four-element array with vertically polarized radiation are presented using the substrate integrated waveguide (SIW) technology. The SIW functions as driven element to generate vertically polarized wave. Microstrip patches are connected to ground plane function as magnetic dipole directors. With this arrangement, a compact magnetic Yagi antenna with vertically polarized radiation is designed. The total area is only $1.58\lambda_1 \times 0.95\lambda_1$ (λ_1 represents the wavelength at 9.5 GHz) and reduced by 63.1% compared to previous magnetic Yagi antenna. The relative bandwidth is 16.15% and peak gain $7.31 \sim 8.82$ dBi. Then the four-element linear array is analyzed, fabricated and measured. Simulated and experimental results demonstrate that the array antenna still preserves vertical polarization, and the peak gain is $14.06 \sim 14.78$ dBi in the relative bandwidth of 14.43%.

1. INTRODUCTION

Yagi antennas have been widely used in wireless communication due to high directivity, simple structure and other advantages. The quasi-Yagi antenna is a kind of printed Yagi antenna, which has low profile, high gain and simplicity in fabrication. It can provide an ultra-wide band using different feed structures [1–3]. However, these antennas only generate horizontal polarization and cannot work conformal to metal plane. In consideration of the image field caused by the relatively large metal surface of antenna carrier, vertical polarization is preferred since it suffers less attenuation loss than horizontal polarization. In application, the conventional Yagi antenna, which is based on electric dipoles, should be placed perpendicular to the metal surface, so that it can operate normally. But this method increases the profile height dramatically. Differently, microstrip Yagi antennas can provide circular or liner polarization (including the vertical polarization) with a large ground plane [4–6]. However, the beam direction cannot point at the end-fire direction. Recently, a microstrip magnetic dipole Yagi antenna with endfire radiation and vertical polarization was proposed in [7]. The antenna was composed of several half-width microstrip lines which works in the EH_1 mode and produced vertically polarized radiation in the end-fire direction. Nevertheless, the feed structure leads to a large antenna size. The length of each element is greater than one wavelength, and the antenna has a large total area of $2.11\lambda_2 \times 1.93\lambda_2$ (λ_2 represents the wavelength at 5.27 GHz).

The substrate integrated waveguide (SIW) has been proposed as a promising technology for microwave and millimeter-wave components achieving low cost, planar, compact, and high-density integration. It has been used as feed structure to realize the antenna miniaturization in the design of antipodal linearly tapered slot antenna [8], and log-periodic dipole array (LPDA) antenna [9]. In order to meet the challenges of microstrip magnetic Yagi antenna with small size, high gain and vertical polarization, a compact magnetic Yagi antenna is presented based on the substrate integrated waveguide (SIW) technology in this letter. The SIW is used as driven element to generate vertically polarized

Received 9 September 2015, Accepted 23 October 2015, Scheduled 27 October 2015
* Corresponding author: Zhao Zhang (bjzhangzhao323@126.com).
The authors are with the Information and Navigation College, Air Force Engineering University, Xi'an 710077, China.

radiation under fundamental mode, and plated through holes is introduced to improve impedance matching. Benefited from the high integration of SIW, the total area of the proposed antenna is $1.58\lambda_1 \times 0.95\lambda_1$ (λ_1 represents the wavelength at 9.5 GHz) and reduced by 63.1% compared to previous magnetic Yagi antenna. Furthermore, to the best of our knowledge, most of the proposed Yagi antennas focus on the bandwidth expansion and gain enhancement. Very few researches on the magnetic Yagi array with vertical polarization have been published. Then we designed four-element Yagi array based on the compact magnetic Yagi antenna. Results shows that the magnetic Yagi array preserves the vertically polarized radiation and tilted beam, and the peak gain is $14.06 \sim 14.78$ dBi. With vertical polarization, high gain and compact configuration, the proposed antenna and array are potentially suitable for the wireless communication.

2. UNIT ANTENNA DESIGN AND ANALYSIS

Figure 1 shows configuration of the proposed magnetic Yagi antenna. All the metal patches are printed on the upside of the RT/duroid 5880 substrate (thickness is 1 mm and $\varepsilon_r = 2.2$), and the downside is a copper ground plane. The SIW is fed by microstrip line, and it works as a driven element to generate vertical polarization under fundamental mode. Its width W_s determines the cutoff frequency of SIW as well as the working band of the proposed antenna. Between the microstrip line and SIW is a tapered microstrip line used to transform the quasi-TEM mode of the microstrip into the quasi-TE_{10} mode in the SIW [10]. Along the microstrip line are two rows of plated through holes (PTHs) which are inserted periodically into the substrate to improve the impedance matching and avoid the leakage of electromagnetic wave. Director elements are rectangular patches. Each one has one short and two long edges connected to the ground plane via PTHs and works as a magnetic dipole director [7]. All the PTHs must meet the equations $0.05 < p/\lambda_c < 0.25$, where p is the distance between PTHs and λ_c the cutoff wavelength, so that they can be equivalent to electric wall and leakage losses are negligible. Between the driven element and the first director, a coupling microstrip patch is placed to improve the impedance matching and to propagate the guided wave to director elements [11]. Since the feed and driven structure, including SIW, ground plane, two rows of PTHs, microstrip and tapered lines, is like an E-plane horn which has high directivity, the reflector elements in conventional Yagi antenna are replaced by the above structure.

Parameter analysis was conducted using Ansoft HFSS. It is found that adding more than two director elements result in a slight increase of the peak gain and the main beam is closer to the end-fire

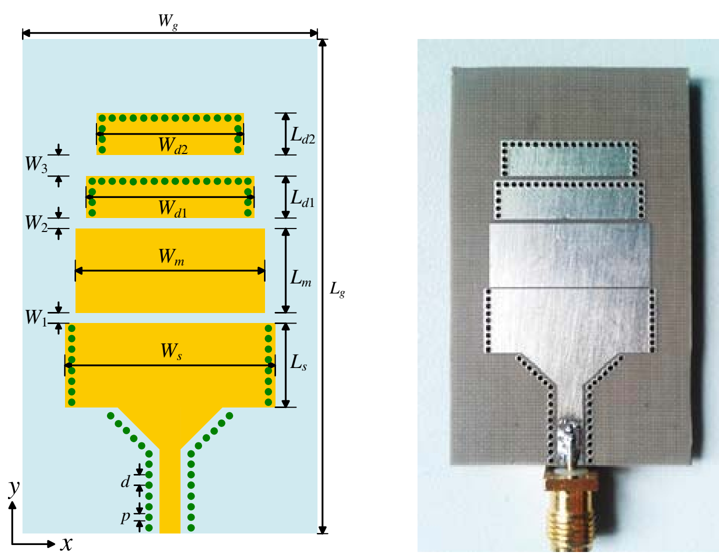

Figure 1. Configuration of the proposed antenna, (a) top view, (b) photo of the fabricated antenna.

Table 1. Parameters of the proposed antenna (Unit: Millimeters).

Parameters	W_s	W_s	W_{d1}	W_{d2}	W_g	W_1	W_2	W_3
Value	21.5	20	17	16	30	0.12	0.4	0.9
Parameters	L_s	L_m	L_{d1}	L_{d2}	L_g	d	p	
Value	8	8	5	4.6	50	0.6	0.9	

direction than that for the proposed Yagi antenna. These results agree with the experimental results obtained in [7]. So only two directors are designed in Fig. 1 and the optimized dimensions are listed in Table 1. It can be seen that the length of driven element (W_s) is $0.68\lambda_1$ and the total area of antenna is only $1.58\lambda_1 \times 0.95\lambda_1$. Obviously the proposed antenna has a compact structure.

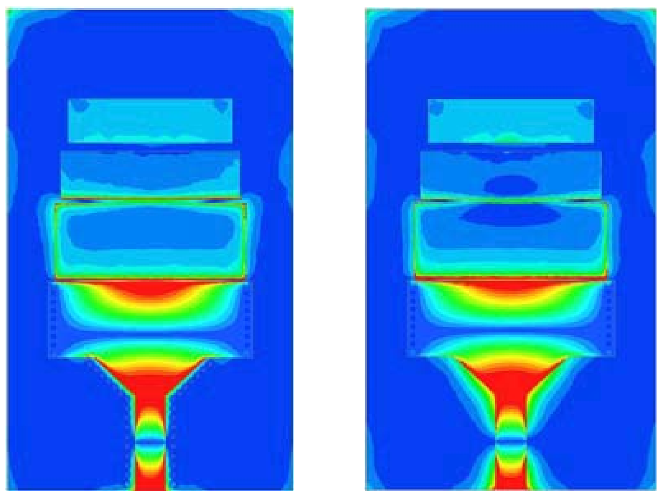

(a) (b)

Figure 2. Comparison of the electric field distribution between the proposed antenna and the one without PTHs, (a) with PTHs, (b) without PTHs.

Figure 2(a) shows the electric field distribution of the proposed antenna at 9.5 GHz. The toroidal electric field of guided wave is excited in the SIW and propagates toward the directors. Fig. 2(b) shows the electric field distribution of the same antenna but without the two rows of PTHs along the feedline. From the field comparison, we can find that the PTHs along the feedline restrict the electric field in the passageway made up by ground plane, microstrip and tapered lines. That is to say, the leakage loss or the leaky wave radiation is suppressed and cross polarization can be reduced [12].

According to the numerical analysis in [13], the surface impedance η of the two rows of PTHs can be defined as $\eta = 0.25\mathrm{j}\omega\mu p \ln(p/2d)$. For the case of $d > p/2$, the surface impedance η of the PTHs is capacitive. The PTHs in the proposed antenna is just this case. In order to verify the improvement of impedance matching caused by the two rows of PTHs, the corresponding comparison of equivalent impedances is shown in Fig. 3. Obviously, the capacitive character is improved, and the imaginary part of the equivalent impedance is decreased for the proposed antenna with PTHs, while the real part of the equivalent impedance almost remains unchanged. Numerical analysis and simulation results are in good agreement. This phenomenon confirms that the impedance matching can be improved by the PTHs along the feedline.

The simulated and measured reflection coefficients S_{11} and peak gains are shown in Fig. 4. The bandwidth of $S_{11} < -10\,\mathrm{dB}$ is $8.7 \sim 10.3$ GHz (the relative bandwidth is 16.84%) for simulation and $8.88 \sim 10.44$ GHz (the relative bandwidth is 16.15%) for measurement. In the working band, the peak gain is $7.26 \sim 8.98$ dBi for simulation and $7.31 \sim 8.82$ dBi for measurement. It can be seen from the plots that the experimental results are in good agreement with the numerical simulations.

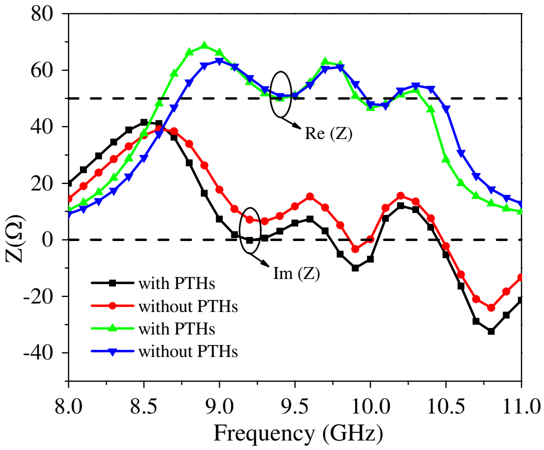

Figure 3. Comparison of equivalent impedances between the proposed antenna with and without PTHs.

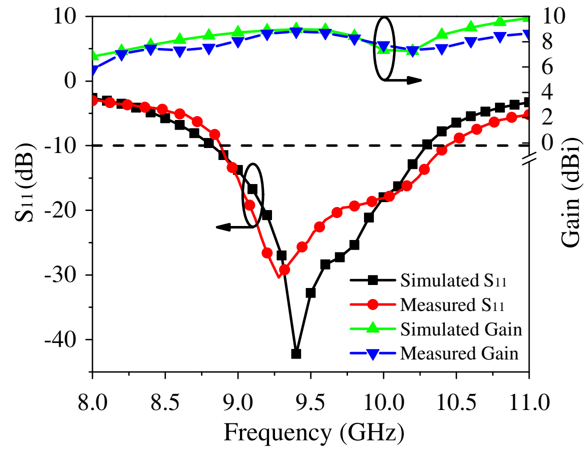

Figure 4. Simulated and measured S_{11} and peak gain of the proposed antenna.

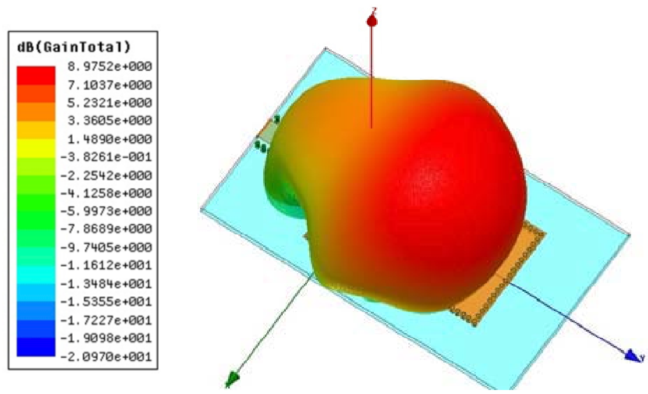

Figure 5. Simulated 3-D radiation pattern at 9.5 GHz.

Figure 5 shows the simulated 3-D radiation pattern at 9.5 GHz. It shows that the antenna has a tilted beam and that the peak gain direction points toward the low elevation direction. Fig. 6 presents the simulated and measured radiation patterns at 9.5 GHz in elevation plane (yoz plane) and azimuth plane (xoy plane). In elevation plane, the co-polarization is vertical polarization, and the peak gain direction occurs at 30°. Within the direction of $0° \sim 90°$, the cross polarization is lower than -47 dB, and the cross polarization isolation is greater than 43 dB. In azimuth plane, the main beam occurs at the end-fire direction, and the F/B ratio (the ratio of the radiation at forward end-fire to that at backward end-fire) is greater than 10 dB. The cross polarization isolation is greater than 15 dB between $85° \sim 95°$, and the maximum reaches 30 dB at 90°.

3. FOUR-ELEMENT ARRAY DESIGN AND ANALYSIS

To demonstrate the performance of magnetic Yagi array, a four-element Yagi array antenna is designed by placing four antennas perpendicular to the main beam direction. Fig. 7(a) shows the configuration of the fabricated array antenna using the common printed circuit method. The feedlines of four elements are directly connected to the quartering power divider network, and the two rows of PTHs along each feedline are preserved. Since all the PTHs in the array are equivalent to electric walls, the mutual coupling mainly depends on the distance between the coupling microstrip patches which has no PTHs. The optimized parameter dx is 26 mm ($0.82\lambda_1$) which is slightly greater than the width W_s of SIW ($0.68\lambda_1$). The total area of the array antenna is $3.42\lambda_1 \times 2.63\lambda_1$. The array antenna was measured in a microwave anechoic chamber as shown in Fig. 7(b). A vector network analyzer (Agilent N5230C) and a linearly polarized standard-gain horn antenna ($2 \sim 18$ GHz) were used to constitute test system.

The simulated and measured S_{11} and peak gains are shown in Fig. 8. The simulated bandwidth is $8.8 \sim 10.3$ GHz (the relative bandwidth is 15.71%), and the peak gain varies between 14.08 dBi and 15.19 dBi in the working band. Measured results show that the bandwidth is $9.0 \sim 10.4$ GHz (the relative bandwidth is 14.43%), and the peak gain varies between 14.06 and 14.78 dBi in the working band. Compared with the results of unit antenna, the peak gain increases more than 6 dBi while the bandwidth keeps almost unchanged. In view of the fabrication and measurement tolerance, the good agreement between simulated and measured results indicates that the four-element linear array can increase the peak gain markedly and the bandwidth keeps unchanged.

The simulated and measured radiation patterns are presented in Fig. 9. From this plot, it is observed that the four-element array still has the characteristics of vertical polarization and tilted beam. The peak gain direction at 9.5 GHz occurs at 46°. The four-element array also exhibits a better performance of cross polarization and F/B ratio. In elevation plane, the cross polarization is lower than −55 dB. Due to the measurement tolerance, the simulated cross polarization isolation is greater than 50 dB while the measured one is only greater than 45 dB within the direction of $0° \sim 90°$. In azimuth plane, the cross polarization isolation is greater than 20 dB between $85° \sim 95°$, and the maximum reaches 52 dB at 90°. A better F/B ratio can be obtained, although the measured result has a slightly lower F/B ratio (13 dB) in comparison to simulation (16 dB).

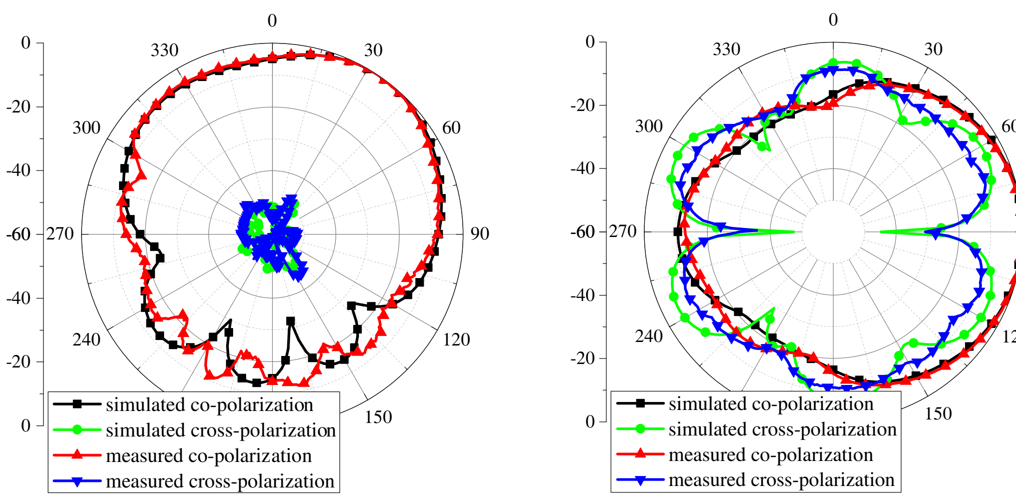

(a) (b)

Figure 6. Simulated and measured radiation patterns at 9.5 GHz, (a) elevation plane, (b) azimuth plane.

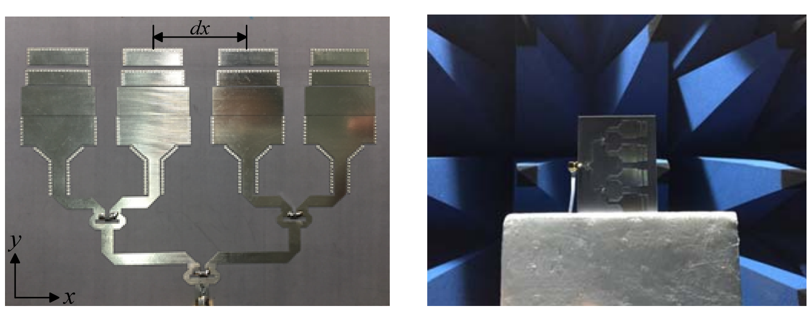

(a) (b)

Figure 7. Photos of the four-element array antenna, (a) configuration of the array antenna, (b) measurement in a microwave anechoic chamber.

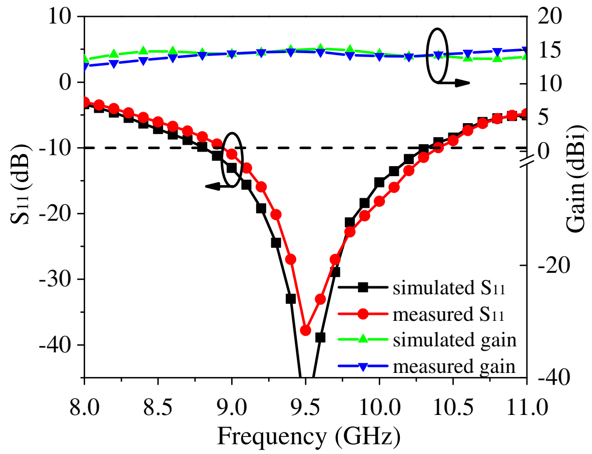

Figure 8. Simulated and measured S_{11} and peak gain of the four-element array antenna.

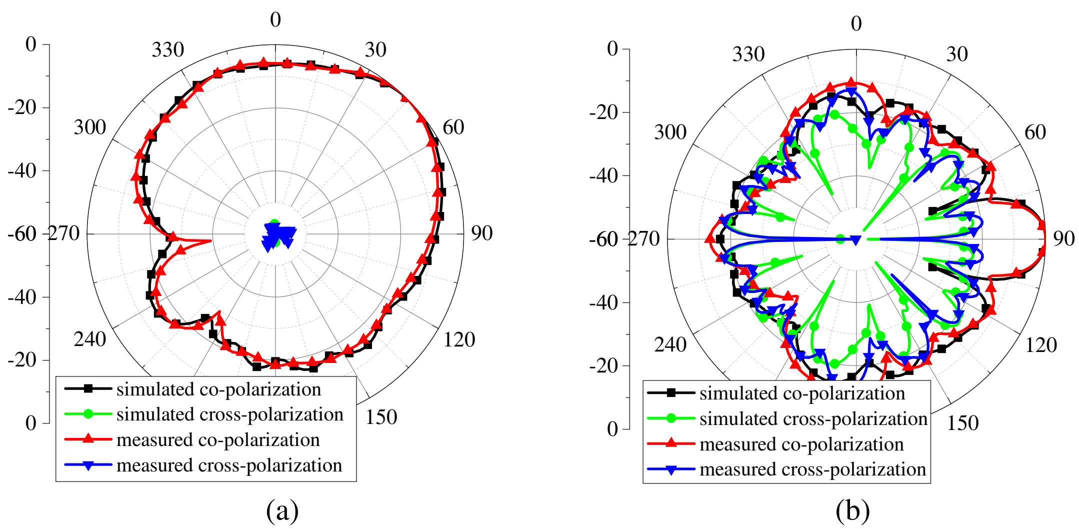

Figure 9. Simulated and measured radiation patterns at 9.5 GHz, (a) elevation plane, (b) azimuth plane.

4. CONCLUSION

In this paper, a microstrip magnetic Yagi antenna with small size, high gain and vertical polarization is presented. The SIW has been utilized to generate vertically polarized wave and realize the miniaturization. The introduction of PTHs along the feedline improves the impedance matching and cross polarization isolation. Good agreement between simulation and measurement indicates that the proposed antenna has a compact size of $1.58\lambda \times 0.95\lambda$ and vertically polarized radiation. The peak gain is $7.31 \sim 8.82$ dBi in the working band $8.7 \sim 10.3$ GHz. Furthermore, the four-element magnetic Yagi array antenna has been analyzed and measured. Experimental results show that the array antenna preserves vertical polarization, and the gain is $14.06 \sim 14.78$ dBi. In addition, the cross polarization isolation and F/B ratio have been enhanced obviously. As a wideband feed structure, SIW has the potential to broaden the antenna bandwidth. However, the coupling patch is a single resonant structure which restricts the impedance matching with the SIW. So the next work should focus on the design of multi-resonant or wide band coupling patch.

ACKNOWLEDGMENT

This work was supported by the National Natural Science Foundation of China under Grant No. 61271100, No. 61471389 and No. 61501494, and the Doctoral Foundation of Air Force Engineering University under Grant No. KGD080914002.

REFERENCES

1. Estrada, J. G., C. I. Páez, and A. Fajardo, "A new broadband quasi Yagi-Uda antenna with an EBG-truncated ground plane," *IEEE Antennas Wireless Propag. Lett.*, Vol. 12, 1392–1395, 2013.
2. Nguyen, P. T., A. Abbosh, and S. Crozier, "Wideband and compact quasi-Yagi antenna integrated with balun of microstrip to slotline transitions," *Electron. Lett.*, Vol. 49, No. 2, 88–89, 2013.
3. Abbosh, A., "Ultra-Wideband quasi-Yagi antenna using dual-resonant driver and integrated balun of stepped impedance coupled structure," *IEEE Trans. Antennas Propag.*, Vol. 61, No. 7, 3885–3888, 2013.
4. DeJean, G. R. and M. M. Tentzeris, "A new high-gain microstrip Yagi array antenna with a high Front-to-Back (F/B) ratio for WLAN and millimeter-wave applications," *IEEE Trans. Antennas Propag.*, Vol. 55, No. 2, 298–304, 2007.
5. DeJean, G. R., T. T. Thai, S. Nikolaou, and M. M. Tentzeris, "Design and analysis of microstrip Bi-Yagi and quad-Yagi antenna arrays for WLAN applications," *IEEE Antennas Wireless Propag. Lett.*, Vol. 6, 244–248, 2007.
6. Honma, N., T. Seki, K. Nishikawa, K. Tsunekawa, and K. Sawaya, "Compact six-sector antenna employing three intersecting dual-beam microstrip Yagi-Uda arrays with common director," *IEEE Trans. Antennas Propag.*, Vol. 54, No. 11, 3055–3062, 2006.
7. Liu, J. and Q. Xue, "Microstrip magnetic dipole Yagi array antenna with endfire radiation and vertical polarization," *IEEE Trans. Antennas Propag.*, Vol. 61, No. 3, 1140–1147, 2013.
8. Cheng, Y. J. and Y. Fan, "Millimeter-Wave miniaturized substrate integrated multibeam antenna," *IEEE Trans. Antennas Propag.*, Vol. 59, No. 12, 4840–4844, 2011.
9. Zhai, G., Y. Cheng, Q. Yin, L. Chiu, S. Zhu, and J. Gao, "Super high gain substrate integrated clamped-mode printed log-periodic dipole array antenna," *IEEE Trans. Antennas Propag.*, Vol. 61, No. 6, 3009–3016, 2013.
10. Deslandes, D. and K. Wu, "Integrated microstrip and rectangular waveguide in planar form," *IEEE Microw. Wireless Component Lett.*, Vol. 11, No. 2, 68–70, 2001.
11. Esquius-Morote, M., B. Fuchs, J. Zürcher, and J. R. Mosig, "A printed transition for matching improvement of SIW horn antennas," *IEEE Trans. Antennas Propag.*, Vol. 61, No. 4, 1923–1930, 2013.
12. Li, S., J. Gao, X. Cao, Z. Zhang, and D. Zhang, "Broadband and high-isolation dual-polarized microstrip antenna with low radar cross section," *IEEE Antennas Wireless Propag. Lett.*, Vol. 13, 1413–1416, 2014.
13. Che, W., K. Deng, D. Wang, and Y. L. Chow, "Analytical equivalence between substrate-integrated waveguide and rectangular waveguide," *IET Microw. Antennas Propag.*, Vol. 2, No. 1, 35–41, 2008.